



## ORIGINAL PAPER

**FEASIBILITY ANALYSIS OF UTILITY SATELLITE ALTIMETRY AND TIDE GAUGES FOR VERTICAL LAND MOTION ESTIMATION ALONG THE COASTLINE OF AUSTRALIA**

Haodong LIU, Xiaoxing HE \*, Shengbo YANG, Jie WANG, Xiang LIU and Raihana ABBASI

*School of Civil and Surveying & Mapping Engineering, Jiangxi University of Science and Technology, Ganzhou 341000, China**\*Corresponding author's e-mail: xxh@jxust.edu.cn***ARTICLE INFO****Article history:**

Received 14 October 2024

Accepted 19 November 2024

Available online 12 December 2024

**Keywords:**

Vertical Land Motion

Satellite Altimetry

Tide Gauges

GNSS

Consistency Analysis

**ABSTRACT**

Accurately monitoring vertical land motion (VLM) near coasts and understanding its spatial and temporal variability is crucial for quantifying its impact on water-land interactions. VLM can be estimated from the global navigation satellite system (GNSS) time series, but only a few tide gauges (TGs) are equipped with a GNSS receiver. TG records encompass relative sea level (RSL) change and VLM, while satellite altimetry (SA) provides absolute sea level (ASL) change in the Earth's center-fixed frame. Accordingly, the difference between these two observations can be used to estimate geocentric VLM along the coasts (altimetry-minus-TG, ALT-TG). This paper addresses the temporal correlated noise in time series to reduce its effect on sea level estimation. Firstly, we analyze the ASL trends at 13 Australian sites using the optimal stochastic noise model from 1993-2021. The mean ASL trend is found to be  $3.01 \pm 0.75$  mm/a from SA, and the mean RSL trend is  $4.61 \pm 2.00$  mm/a, and it shows a good consistency of existing research of White et al. (2014) with  $3.40 \pm 0.40$  mm/a (ASL) and  $4.50 \pm 1.30$  mm/a (RSL). Secondly, the estimated GNSS trend shows a good agreement with NGL/SONEL solutions, and we utilized the weighted VLM as a reference to ALT-TG estimation. Thirdly, our study shows that the standard deviation (SD) of the VLM difference between ALT-TG and GNSS is 0.46 mm/a (the VLM difference typically between  $\sim \pm 0.12$ – $1.68$  mm/a), which indicates that it is possible to utilize SA and TG data for VLM estimation along the coastline of Australia. Furthermore, we investigate the accuracy of ALT-TG inversion for VLM and its influencing factors. Our findings indicate that, in regions with high observation quality and reliable data sources, the length of the overlapping period between TG and GNSS observations is the most critical parameter affecting the consistency of trend between the two technologies.

**1. INTRODUCTION**

Vertical land motion (VLM) has become a prominent issue in studies of sea level rise over the past several decades to century timescales (Church et al., 2013; Wöppelmann et al., 2016; Harvey et al., 2021; Hammond et al., 2021; Oelmann et al., 2024). VLM is also a key element in understanding how sea levels have changed over the past century and how future sea levels may impact coastal areas (Wöppelmann and Marcos, 2016). Several studies showed that prolonged land subsidence and ongoing sea level rise in coastal areas pose significant threats to the ecological environment and human life, garnering substantial attention from scholars worldwide (Brown et al., 2013; Takagi et al., 2016; Wang et al., 2018; Denys et al., 2020; Tay et al., 2022; Li et al., 2024). Therefore, it is important to study VLM in coastal zones.

Traditionally, precise leveling was used to measure VLM at coastal tide gauge (TG) stations. This method is with high accuracy (Lyon et al., 2018). However, it faces limitations such as low efficiency and unable to obtain long-term continuous observations, hindering its widespread use. With

advancements in Global Navigation Satellite System (GNSS) technology, methods using continuous GNSS observations to precisely measure land subsidence have rapidly developed. Numerous studies (Bos et al., 2014; Montillet et al., 2018; He et al., 2022; Qiao et al., 2023) have used continuous GNSS data to study VLM at TG stations along the coastline. However, the limited availability of coastal GNSS stations hindered further application in monitor coast VLM. According to Wöppelmann and Marcos (2016) only 14% of the Global Sea Level Observing System (GLOSS) TG have co-located GNSS stations, and these stations have a relatively short temporal coverage (averaging about 10 years). In addition, several studies have demonstrated that InSAR (Interferometric Synthetic Aperture Radar) technology is possible for area land motion monitoring (Grgić et al., 2020; Kowalczyk et al., 2021). Moreover, coastal regions are influenced by sea level fluctuations and multi-path effects, which pose significant challenges for GNSS VLM monitoring. Consequently, comprehensive studies utilizing GNSS observation to analyze VLM at TG stations and their surrounding areas remain limited (King et al., 2012; Santamaría-Gómez et al., 2012;

Watson et al., 2015; Pfeffer et al., 2016). Additionally, several studies are using Glacial isostatic adjustment (GIA) models to compare with the estimated VLM to understand from where the VLM originates (Church et al., 2011; Peltier et al., 2015). However, GIA models are intricate, involving VLM and various geophysical processes. Accurately isolating VLM continues to pose challenges. Current GIA methods primarily rely on model inversion, with the accuracy of these models directly affecting the reliability of GIA estimates. Predictive models, including GIA models, face challenges due to inadequate parameter constraints, which limit their accuracy and fail to account for local processes (King et al., 2010).

An alternative approach to estimating VLM along the coast is based on differencing the altimeter and TG data (ALT-minus-TG, ALT-TG). TG records include relative sea level (RSL) changes and potential VLM (Church and White, 2006; Santamaría-Gómez et al., 2014; Hay et al., 2015; Avsar et al., 2016; Thompson et al., 2016; Kleinherenbrink et al., 2018), while satellite altimetry (SA) offers absolute sea level (ASL) changes within a geocentric reference frame (Rovere et al., 2016; Passaro et al., 2021). The difference between these two techniques can be used to estimate geocentric VLM in coastal areas. Over the years, advancements in SA have enabled this method to derive VLM (Cazenave et al., 1999; Pfeffer et al., 2016; Oelmann et al., 2022). Nonetheless, the ALT-TG method for inferring coastal VLM presents certain challenges: 1) accuracy near the coast and noise amplitude persist in ALT-TG (Adebisi et al., 2021; Oelmann et al., 2022). 2) lack of strict temporal synchronization between SA and TG. 3) temporal autocorrelations in geophysical records is well known and may lead to a significant underestimation of the uncertainties in linear trends (Williams et al., 2003; Hughes et al., 2010; Bos et al., 2014.) Thus, the ALT-TG method for inversion of VLM lacks systematic and reliable studies.

In this work, we assess the feasibility of using SA and TG data to estimate VLM along the Australia's coastline, and explore the reliability of the ALT-TG method for inverse VLM. The remainder of the paper is organized as follows. Section 2 briefly describes the SA Data, TG Data, GNSS Height time series and related model we used in this analysis. Section 3 we analyzed absolute and relative sea level changes along Australia's coastline, used the ALT-TG method to estimate VLM, and compared the results with GNSS results. Finally, concluding remarks are given in Section 4.

## 2. DATA AND METHOD

### 2.1. SATELLITE ALTIMETRY DATA FROM CMEMS

SA has provided high quality, near-global measurements of sea-surface height (SSH) since 1993 (Beckley et al., 2010; Ribal et al., 2019). SSH products based on SA, which has an accuracy of 2~3 cm with respect to an Earth-fixed reference frame (Fu and Cazenave, 2000). In this work, we use the copernicus

marine global reanalysis product GLOBAL\_MULTIYEAR\_PHY\_001\_030 (with access

[https://data.marine.copernicus.eu/product/GLOBAL\\_MULTIYEAR\\_PHY\\_001\\_030/](https://data.marine.copernicus.eu/product/GLOBAL_MULTIYEAR_PHY_001_030/)) from the Copernicus Marine Environment Monitoring Service (CMEMS), GLOBAL\_MULTIYEAR\_PHY\_001\_030 is defined on a standard regular grid at 1/12 degree resolution and covering approximately 8 km (He et al., 2022). The goal of the copernicus marine global ocean reanalysis is to provide an eddy resolving global ocean simulation, covering the recent period during which altimeter data is available, e.g., sea surface height and sea-ice features (Taburet et al., 2019; He et al., 2022). we determined the 13 virtual coastal stations based on the longitude and latitude of the selected coastal Australia TG. Figure 1 and Table 1 showed the detailed information of the virtual coastal stations with SA observations and the SSH time series are processed with the open-source software SA\_Tool V1.0 (Huang et al., 2024).

### 2.2. TIDE GAUGE DATA FROM PSMSL

In this work the monthly tide gauge data were downloaded from the Permanent Service for Mean Sea Level website (Holgate et al., 2013; <https://psmsl.org>). The monthly files list the date (year-month in decimal form) and the average monthly mean sea level value (Huang et al., 2024). In order to compare the feasibility of utilize satellite altimetry and tide gauges to determine the vertical land motion, we try to restricted the time span of SA, TG and GNSS time series with the same time period of 1993.0 to 2021.0, and in Table 1 we provide information about the corresponding analyzed sites, including their latitude and longitude, data gap rates, distances between the sites, and the overlap between different datasets.

### 2.3. GNSS HEIGHT TIME SERIES

The GNSS time series used in this study were acquired from Nevada Geodetic Laboratory (NGL, Blewitt et al., 2018; Hammond et al., 2021; <http://geodesy.unr.edu>). GNSS is a commonly used geodetic technique due to its high precision to monitor land motions (Jin et al., 2007).

Ideally, the reference points of the different techniques should be located as closely as possible to increase the chances that the sensed environment presents homogeneous conditions. In addition, the representativeness of the observations increases with the length of the overlapping interval among the three techniques. The identification of a suitable dataset is a challenging endeavor that requires considering and inspecting several databases and setting reasonable rejection thresholds. Among the most common issues, TG observations typically do not cover the whole altimetry era and GNSS time series often overlap just marginally with those provided by the TG. finally, we could identify 13 sites for inter-technique comparisons.

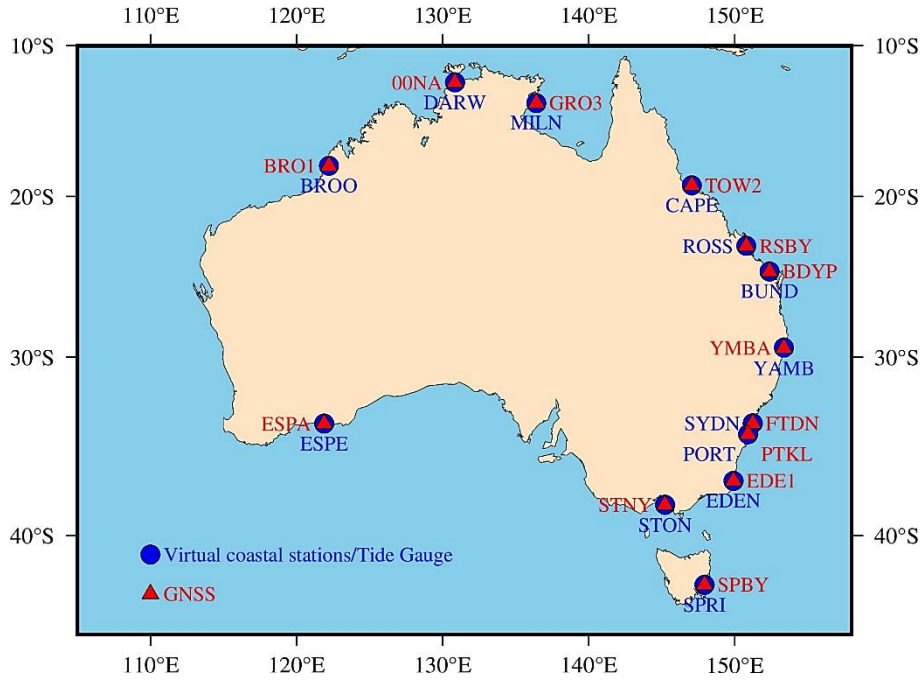


**Fig. 1** Spatial distribution of the analyzed 13 virtual coastal stations/TG/GNSS stations in this work (blue for virtual coastal stations/TG and red for GNSS).

**Table 1** Information of SA, TG and co-located GNSS used in this work.

Tide Gauge 1993~2022)	Lat.	Lon	Data Gap (%)	Co- located GNSS	Data Span	Distance (km)	TG&GNSS Overlap (%)	Virtual coastal- satellite altimetry station
SYDNEY	-33.86	151.23	0.56	FTDN	2012.41-2023.58	0.06	36.66	The virtual SA time series is processed with SA_Tool V1.0 toolbox (Huang et al., 2024) based on the lon and lat of analyzed TGs. All SA products are in time span 1993.0~2021.0 (with no data gap).
YAMBA	-29.43	153.36	3.06	YMBA	2012.61-2024.38	2.01	38.24	
PORT KEMBLA	-34.47	150.91	0.28	PTKL	2009.73-2024.38	0.26	45.33	
EDEN	-37.07	149.91	2.50	EDE1	2014.96-2024.38	0.26	30.20	
DARWIN	-12.47	130.85	0.00	00NA	2008.24-2018.73	0.61	29.54	
STONY POINT	-38.37	145.23	2.50	STNY	2011.41-2021.93	0.99	34.92	
ESPERANCE	-33.87	121.90	0.83	ESPA	2008.45-2024.38	0.39	48.49	
BUNDABERG	-24.77	152.38	0.00	BDYP	2016.67-2020.32	0.59	10.87	
BROOME	-18.00	122.22	0.00	BRO1	2010.52-2024.38	1.07	43.49	
MILNER BAY	-13.86	136.42	3.61	GRO3	2017.83-2024.38	0.73	20.35	
SPRING BAY	-42.55	147.93	0.28	SPBY	2008.77-2024.38	0.17	49.46	
CAPEFERGUSO	-19.28	147.06	1.39	TOW2	1995.39-2024.38	0.94	92.73	
ROSSLYN BAY	-23.16	150.79	1.11	RSBY	2011.57-2024.38	0.01	31.82	

**2.4. INVERSION OF VLM FROM ALT-TG**

It has been pointed out that VLM can also be Measurement by SA and TG along the coastline (Thompson et al., 2016; Kleinherenbrink et al., 2018). Tide gauge records comprise of relative sea level change and vertical land motion, while satellite altimetry provides absolute sea level change in the Earth’s center fixed frame. Accordingly, the difference of both observations can be used to estimate geocentric vertical land motion along the coasts. Previous studies have shown that sea level time series contain temporal noise. The selection of appropriate

noise model is an important factor of characterizing the nature of noise and reducing the formal error in uncertainty estimates (Royston et al., 2018; Huang et al 2024). We examine stochastic noise with a time-varying seasonal signal from the linear trend estimation of the sea level and GNSS data. We select the autoregressive moving average (ARMA (p, q)), autoregressive fractionally integrated moving average (ARFIMA (p, d, q)), generalized gauss-markov (GGM), flicker and white noise (FNWN), random walk, flicker, and white noise (RWFNWN), and power law and white noise (PLWN) models, following

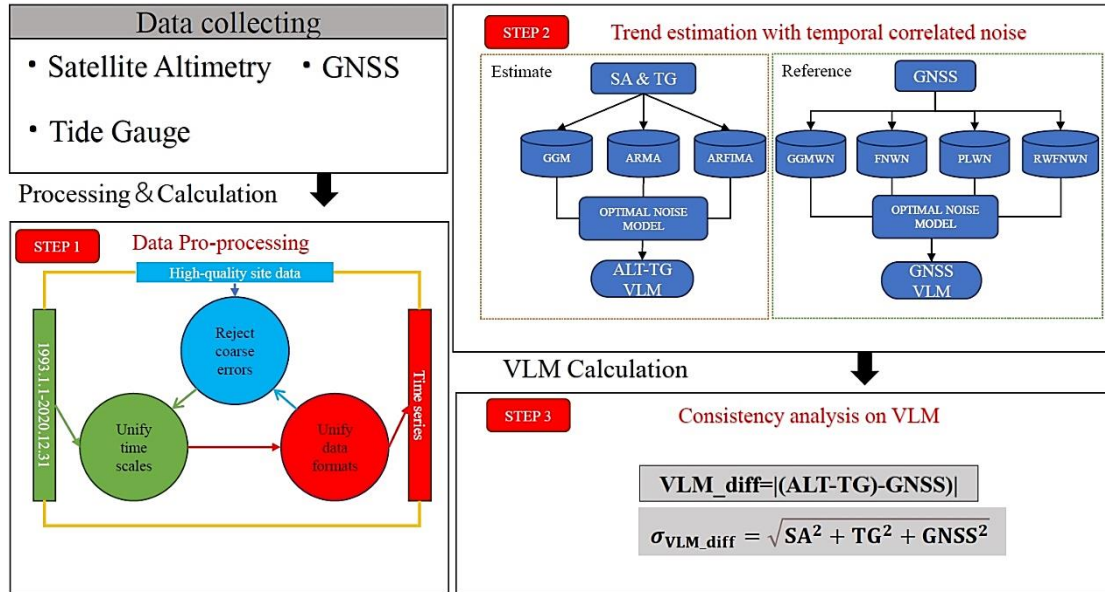


Fig. 2 Flow of ALT-TG for VLM and feasibility analysis.

Montillet et al. (2018), Wöppelmann et al. (2012), and He et al. (2017, 2019), using the package Hector (accessible at <https://teromovigo.com/hector/>). To accurately model the stochastic noise properties of the time series, we employ the optimal noise model selection criterion called BIC<sub>tp</sub>, as described in He et al. (2019). In this paper, first we collect data and pre-process the data, including remove outliers and unify the time scale. It is worth mentioning that due to the short time series of GNSS itself, for a number of sites, GNSS observations overlap with TG ones only for a limited amount of time (see in Table 1). Then we use the GGM, ARMA (p, q), and ARFIMA (p, d, q) models are used to measure the VLM from the ALT-TG method, because the VLM is calculated from the SA and TG respectively. The above models were used to process the SA data and TG data respectively, and the optimal model was selected based on the estimation criterion BIC<sub>tp</sub>, calculate to get the VLM velocity and uncertainty for the corresponding site. For the GNSS time series corresponding to each station, this study employed four common combined noise models: Generalized Gauss Markov+white noise (GGM+WN), white noise + random walk noise + flicker noise (WN+RW+FN), PLWN, and FNWN. Each station's data is processed using the optimal time-varying noise model according to the criterion, ensuring more accurate and reliable velocity estimates. Detailed procedures are provided in Figure 2. Finally, we calculate the difference value of the VLM between the two methods and used this value as a reliance for evaluating whether ALT-TG can invert the VLM in the coastal zone (a difference value of less than 2 mm/a is considered to be more reliable for ALT-TG inversion of VLM at this site) (Nerem and Mitchum, 2002; Ostanciaux et al., 2012; Kleinerherbrink et al., 2018; Watson, 2019; He et al., 2022), and likewise this value can be quantified for the

subsequent analysis of sources of differences in VLM measured by the two methods.

## 2.5. ACCURACY EVALUATION OF VLM BETWEEN ALT-TG AND GNSS

To evaluate the accuracy of the estimated VLM from ALT-TG, we compare the ALT-TG results with GNSS. Previous research indicates that the VLM at TG stations can be accurately estimated using nearby GNSS measurements, we use the GNSS-derived VLM as the reference value and treat the ALT-TG result as the estimated value. By assessing the consistency between these two sets of results, we can evaluate the precision of the ALT-TG method. There are two main issues involved in estimating VLM trends for TGs with GNSS time series. Firstly, many GNSS stations are not directly connected to TG stations. For the definition of TG co-located GNSS stations, previous studies suggest: the distance between the TG and nearest GNSS station should be small enough so that any relative vertical motion is minimized, and GPS antennas less than about 20km from the tide gauge were considered to be co-located (Collilieux et al., 2011). The spatial distance limitation ensures as possible that the GNSS and the TG sites are close enough, and therefore the GNSS vertical motion can directly contribute to the TG-derived trend (velocity) (Collilieux et al., 2011; Bitharis et al., 2017). For comparison, we have analyzed the measurements from a total 13 of GNSS stations which are co-located at or close to a TG station along the Australia (Fig. 1; Table 1), and secondly, we estimate the trend from the GNSS time series, which contains autocorrelation noise signals and offsets that are often undocumented (Blewitt et al., 2016; Hammond et al., 2021). We consider the effect of the noise model on the computed VLM trend, as discussed in Section 2.4.

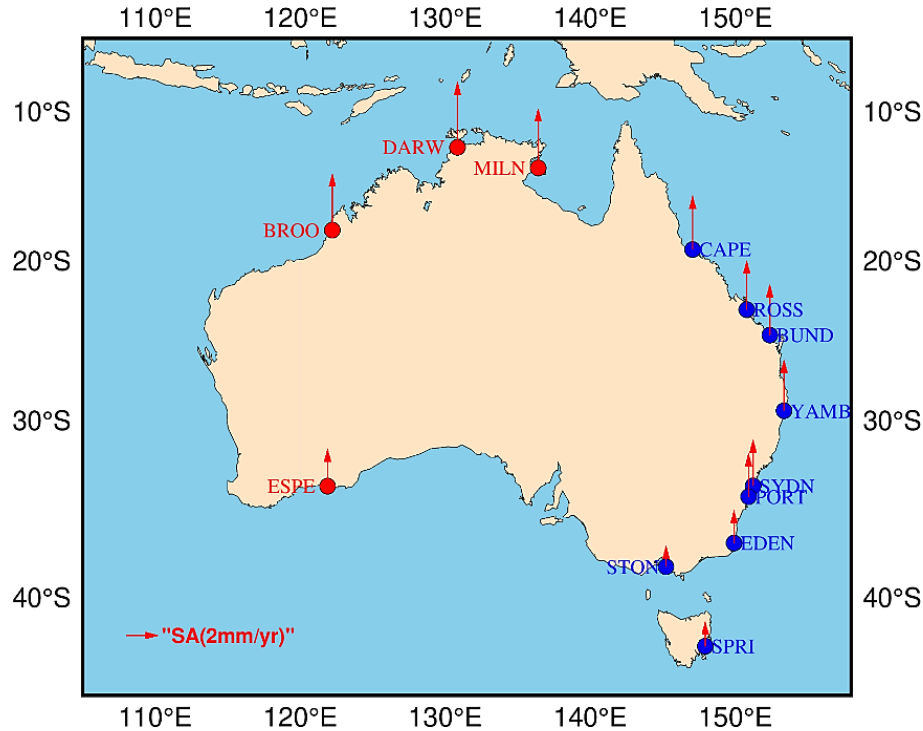


**Fig. 3** Sea level change rate based on SA along the coastline of Australia (Red sites contribute to the west coast of Australia, blue sites contribute to the east coast of Australia).

### 3. RESULT AND ANALYSIS

In this section, we calculate the absolute and relative sea level change around the coastline of Australia. Then, the ALT-TG method is used to invert the VLM of the Australian coastline. Then we compared the estimated GNSS results estimated using the optimal noise model in this study with those provided by different institutions. Finally, the various GNSS estimated trends are weighted and averaged, and compared with the VLM obtained from the ALT-TG method.

#### 3.1. ASL ALONG THE COASTLINE OF AUSTRALIA BASED ON SA

There is no clear geographical pattern for the optimal noise model so by using the optimal point-wise noise model for altimeter and TG data (Peng et al., 2022). As shown by the red arrows in Figure 3, the ASL along the Australian coast is generally on an upward trend. The range of ASL changes along the Australian coast varies from  $1.30 \pm 0.65$  mm/a to  $5.03 \pm 1.15$  mm/a, specifically, and the uncertainties on ASL trends range from 0.43 to 2.13 mm/a, with a median value of 0.58 mm/a. The ASL trends vary across different regions, with a slightly larger increase in the west region ( $4.05 \pm 1.12$  mm/a) compared to the east region ( $2.56 \pm 0.58$  mm/a). Particularly, the ASL at DARWIN ( $5.03 \pm 1.15$  mm/a) and BROOME ( $4.56 \pm 0.63$  mm/a). The mean ASL rate of the

Australian coastline (based on the analyzed 13 sites) is  $3.01 \pm 0.75$  mm/a, and this is consistent with the result of White et al. (2014) (with  $3.40 \pm 0.40$  mm/a from satellite altimeters for 1993-2009).

#### 3.2. RELATIVE SEA LEVEL BASED ON TIDE GAUGE TIME SERIES

RSL along the coast of Australia, as indicated by the blue arrows in Figure 4, is generally on an upward trend. The RSL along the Australian coast varies from  $2.59 \pm 1.07$  mm/a to  $6.46 \pm 3.77$  mm/a and uncertainties on RSL trends are slightly higher (median value = 1.59 mm/a). They exceed 2 mm/a at 4 stations, and high uncertainties ( $>2$  mm/a) are retrieved majorly along the West coast of Australia (Figure 4 red point stations). We conclude that probably due to non-linear variability in pluri-decadal sea level records (Donner et al., 2012; White et al., 2014; Pfeffer et al., 2016). RSL trends are all larger than the ASL trends, reflecting the influence of VLM on all regions. Additionally, the RSL trend in the west region ( $5.83 \pm 3.69$  mm/a) is generally higher than that in the east region ( $4.08 \pm 1.26$  mm/a). This is similar to the ASL trend and also shows a scenario where the average trend is greater in the west than in the east. Furthermore, the RSL trends measured by neighboring TG are similar, which is related to the higher correlation coefficient between neighboring TG stations. The RSL at DARWIN ( $6.46 \pm 3.77$  mm/a) and BROOME ( $6.23 \pm 3.11$  mm/a)

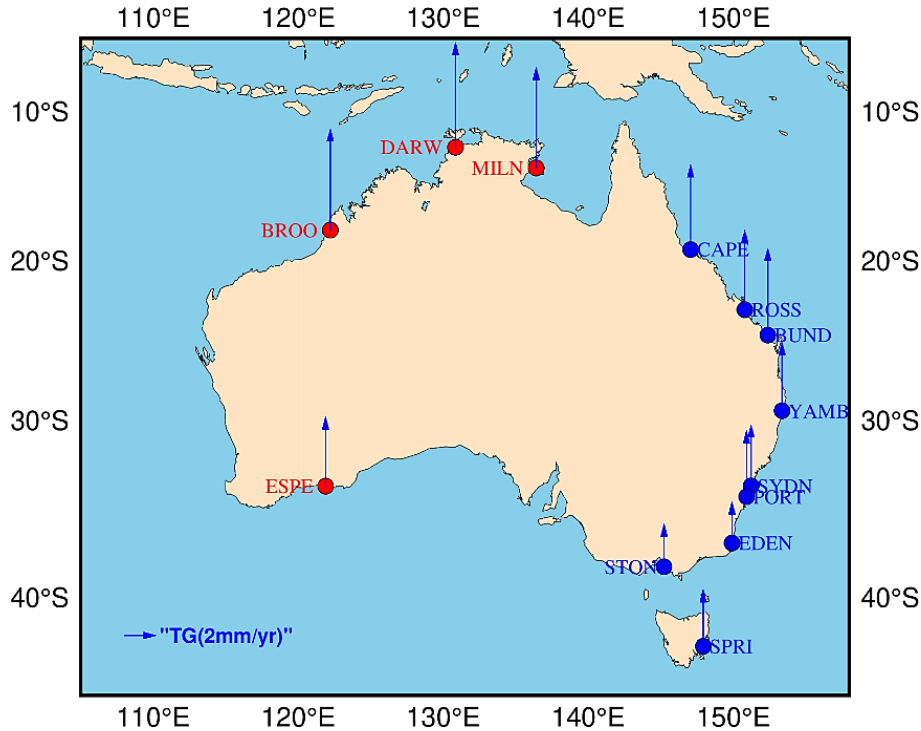


**Fig. 4** Sea level change rate based on TG along the coastline of Australia (Red sites contribute to the west coast of Australia, blue sites contribute to the east coast of Australia).

located along the Australian coast increased much faster than at other sites. The mean RSL rise at the 13 sites along the coast of Australia is  $4.61 \pm 2.00$  mm/a, and this is also consistent with the existed research of White et al. (2014) ( $4.50 \pm 1.30$  mm/a Rates of Australian averaged MSL rise for 1993–2009). Additionally, due to differences in TG site selection and time scales between this study and the referenced works, minor discrepancies are evident in the calculated average sea level change.

### 3.3. INVERSION OF VLM FROM ALT-TG METHOD

To estimate the VLM at the TG stations along the Australian coastline, this study applied the aforementioned optimal noise model to assess the sea level change in Australia. The trend of RSL, ASL and  $VLM_{ALT-TG}$  at the 13 sites over the period 1993–2021 are shown in Table 2. All TGs showed a positive RSL and ASL with a range from 1.30 to 6.46 mm/a. One of the sites is particularly special. In EDEN, the RSL rate was  $2.59 \pm 1.07$  mm/a, and the ASL rate was  $2.04 \pm 0.43$  mm/a. The VLM derived from the difference between these rates was minor, at  $-0.55 \pm 1.15$  mm/a. The VLM results from ALT-TG along the coast of Australia showed that the rate was not spatially uniform. The specific large rates were  $-2.17 \pm 0.96$  mm/a,  $-2.12 \pm 1.81$  mm/a, and  $-2.00 \pm 2.16$  mm/a at TG site SPRING BAY in southeastern Australia, TG site BUNDABERG in the east of Australia and TG site ESPERANCE in southwestern Australia, respectively. The specific low rates were  $-0.55 \pm 1.15$  and  $-0.92 \pm 1.11$  mm/a at

TG sites EDEN and SYDNEY, respectively. The VLM rates from GNSS data also presented similar spatial variation characteristics along the coast of Australia.

In the context of rising sea levels along the Australian coastline, the SPRING BAY TG station exhibited an RSL rise rate of approximately 3.53 mm/a. This contrasts significantly with the rate of 1.53 mm/a derived from SA, suggesting the influence of local factors. It can be preliminarily inferred that the TG station experienced considerable subsidence during the same period. According to SA, the sea level rise rates were 5.03 mm/a for DARWIN and 1.30 mm/a for STONY POINT, while other stations showed an average ASL rise rate of 2.99 mm/a, with a small standard deviation (SD) of 0.87 mm/a. This indicates that the data differences among different stations ASL change rate are minor (Table 2, Column 2). In comparison, after removing one maximum and one minimum value, the RSL change rates calculated from the TG exhibit larger differences. The average RSL rate is 4.63 mm/a, with a SD of 1.10 mm/a (Table 2, Column 3). Since we are only concerned with the variation in VLM, the difference between the ASL rise rates observed by SA and the RSL rise rates observed by TG can be used to derive the VLM rates. This approach disregards the impact of different reference frames. Thus, we can conclude that the primary reason for the discrepancies between SA and TG observations is the influence of VLM on the TG stations. This, in turn, reflects the significant impact of VLM on TG observations in Australia.

**Table 2** Sea Level Rise and Vertical Land Motion at TGs (mm/a).

TG	ASL SA	RSL TG	VLM <sub>ALT-TG</sub>
SYDNEY	2.89±0.44	3.81±1.02	-0.92±1.11
YAMBA	3.16±0.53	4.27±1.78	-1.11±1.86
PORT KEMB	2.70±0.44	4.29±1.01	-1.58±1.10
EDEN	2.04±0.43	2.59±1.07	-0.55±1.15
DARWIN	5.03±1.15	6.46±3.77	-1.43±3.94
STONY POIN	1.30±0.65	2.68±1.15	-1.38±1.32
ESPERANCE	2.33±0.58	4.33±2.08	-2.00±2.16
BUNDABERG	3.15±0.54	5.26±1.73	-2.12±1.81
BROOME	4.56±0.63	6.23±3.31	-1.67±3.37
MILNER BAY	4.29±2.13	6.29±5.61	-1.99±6.00
SPRING BAY	1.36±0.53	3.53±0.80	-2.17±0.96
CAPE	3.34±0.90	5.28±1.59	-1.95±1.83
ROSSLYN	3.06±0.80	4.98±1.19	-1.92±1.43

**Table 3** Rates of VLM measured by different agencies (mm/a).

GNSS	Our		SONEL		NGL		Combined		VLM ALT-TG	
	VLM	$\sigma$	VLM	$\sigma$	VLM	$\sigma$	VLM	$\sigma$	VLM	$\sigma$
FTDN	-1.53	0.66	-1.47	0.55	-1.25	0.52	-1.41	0.58	-0.92	1.11
YMBA	-1.58	0.67	-2.47	0.72	-0.92	0.62	-1.66	0.67	-1.11	1.86
PTKL	-1.34	0.31	-1.21	0.62	-1.38	0.56	-1.31	0.51	-1.58	1.10
EDE1	-1.68	0.71	-1.68	0.34	-1.25	0.58	-1.54	0.56	-0.55	1.15
00NA	-1.05	0.93	-0.96	0.92	-0.98	0.92	-1.00	0.83	-1.43	3.94
STNY	-1.01	0.27	-1.01	0.66	-1.75	0.66	-1.26	0.56	-1.38	1.32
ESPA	-1.27	0.22	-1.02	0.52	-0.94	0.49	-1.08	0.43	-2.00	2.16
BDYP	-0.33	2.47	-0.22	1.15	-0.76	1.52	-0.44	1.80	-2.12	1.81
BRO1	-0.98	0.61	-1.95	0.63	-1.37	0.52	-1.43	0.59	-1.67	3.37
GRO3	-0.69	1.41	-0.69	0.61	-0.11	0.99	-0.50	1.05	-1.99	6.00
SPBY	-1.51	0.16	-1.74	0.52	-1.39	0.48	-1.55	0.42	-2.17	0.96
TOW2	-1.41	0.77	-1.06	0.46	-0.96	0.44	-1.14	0.58	-1.95	1.83
RSBY	-0.62	0.65	-0.83	0.92	-1.03	0.87	-0.83	0.82	-1.92	1.43

### 3.4. VLM DERIVED FROM GNSS TIME SERIED

To validate the accuracy of the ALT-TG measurements, this study calculated the VLM results from GNSS stations located near 13 TG sites. Additionally, to obtain more reliable GNSS results for comparison with the ALT-TG results, further analyses were conducted, we utilized various published VLM solutions derived from GNSS station records for comparative analysis, specifically from Système d'Observation du Niveau des Eaux Littorales (SONEL), <http://www.sonel.org> and NGL. Each solution utilizes different analytical software to determine trends. SONEL provides GPS solutions covering coastal areas as part of the Global Sea Level Observing System (GLOSS) network, based on GNSS data spanning from January 1995 to December 2013 (known as the ULR6a GPS solution). The vertical velocity field is expressed in the International Terrestrial Reference Frame 2008 (ITRF2008), with trends (i.e., velocities and standard errors) determined using the Combination and Analysis of Terrestrial Reference Frame (CATREF) software (Altamimi et

al., 2007; Santamaría-Gómez et al., 2017). NGL collects raw GPS data from more than 17,000 stations globally, providing multipurpose open-access data products (Blewitt et al., 2018) with routine updates to station velocities. These velocities and associated errors are robustly estimated using the Median Interannual Difference Adjusted for Skewness (MIDAS) software, a median-based GPS station velocity estimator that is insensitive to outliers, seasonal effects, abrupt changes from earthquakes or equipment adjustments, and statistical data variability (Blewitt et al., 2016). Various published VLM solutions from GNSS station records were used in this study for comparative purposes, as shown in Table 3.

Figure 5 illustrates the VLM measured by different institutions, and combined with the data from Table 3, it is evident that our GNSS-derived estimates exhibit good consistency with those provided by official agencies. The overall trends across various stations align closely, despite minor discrepancies. For instance, at the FTDN site, our GNSS estimate is -1.53 mm/a, while the SONEL and NGL estimates are

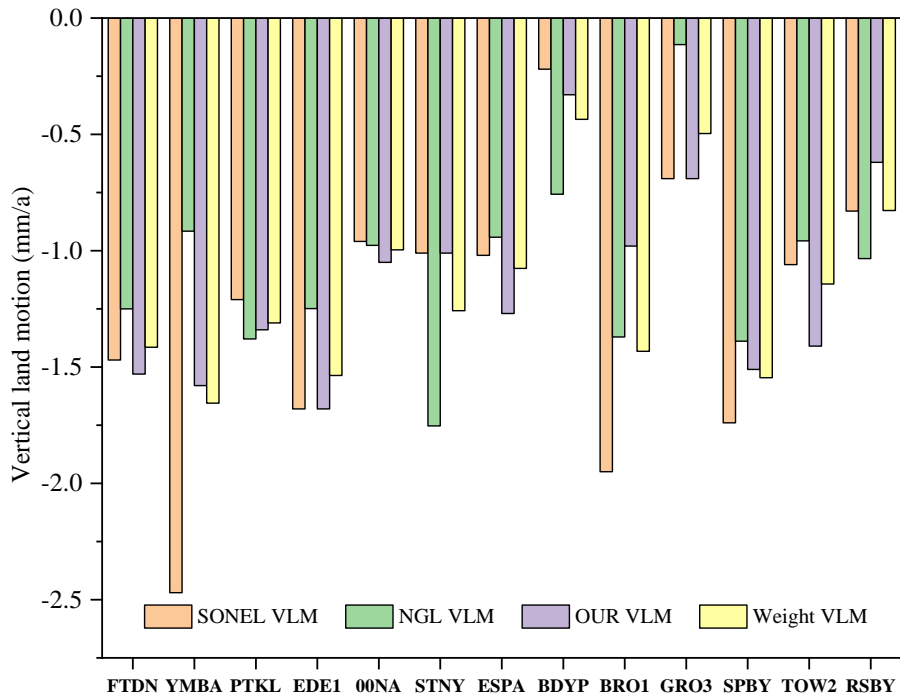


Fig. 5 Vertical Land Motion Rates Measured by Different Institutions.



Fig. 6 The uncertainty of VLM rates measured by different Institutions (The number on the bar graph represent GNSS data time series span/a).

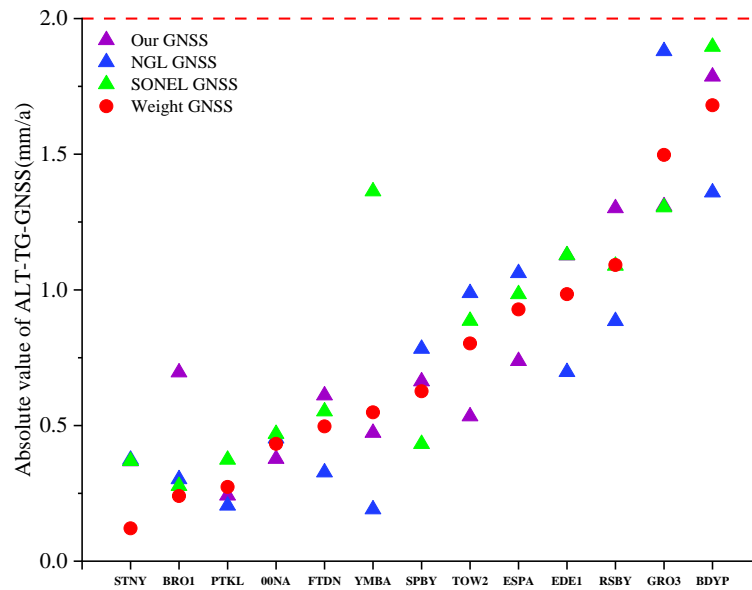


Fig. 7 The Absolute Discrepancy in VLM between ALT-TG and Global Navigation Satellite System Stations.

Table 4 Summary table of difference |ALT-TG minus GNSS|.

GNSS sources	maximum (mm/a)	Average (mm/a)	SD (mm/a)	RMSE (mm/a)
our result	1.79	0.79	0.44	0.90
NGL	1.88	0.73	0.48	0.88
SONEL	1.90	0.86	0.47	0.98
Weight	1.68	0.75	0.46	0.88

-1.47 mm/a and -1.25 mm/a, respectively. This alignment in trends underscores the stability of our GNSS measurements. Additionally, the uncertainties associated with our estimates are comparable to those of the official agencies, further demonstrating the reliability of our methods. At the PTKL site, the uncertainty in our GNSS estimate is 0.31 mm/a, which is within a similar range to SONEL's 0.62 mm/a and NGL's 0.56 mm/a. Such consistency is observed across multiple sites, including YMBA and STNY, where both the VLM rates and uncertainties align well with those from SONEL and NGL. Therefore, the good agreement between our GNSS-derived VLM data and the official data, both in terms of specific rates and associated uncertainties, also reflects the high reliability of GNSS for estimating VLM.

In addition, as shown in Figure 6, we observed a close relationship between the uncertainty of site-specific VLM and the length of GNSS time series. Specifically, GNSS time series spanning over 10 a typically result in VLM uncertainties ranging from 0.5 to 1.0 mm/a. Conversely, shorter GNSS time series, such as those at sites BDYP and EDEI with lengths of 3.7 a and 6.5 a respectively, lead to larger uncertainties in estimated VLM. This suggests that shorter GNSS time series may introduce greater uncertainty in estimating site-specific VLM. Therefore, when comparing the computed VLM

values with those derived from long-term ALT-TG records, discrepancies may arise due to these uncertainties. This is one of the sources contributing to the differences in VLM estimates between the two methods. In the subsequent sections, we will discuss this in detail.

### 3.5. FEASIBILITY ANALYSIS OF UTILITY ALT-TG FOR VLM ESTIMATION

To verify the reliability of the ALT-TG method for inverting coastal VLM, we calculated the absolute differences between the VLM derived from the ALT-TG method and those obtained from three GNSS datasets, including their weighted average (see in Figure 7). The results showed that for the 13 coastal sites, the discrepancies were all within 2 mm/a (Nerem and Mitchum, 2002; Ostanciaux et al., 2012; Kleinherenbrink et al., 2018; Watson, 2019; He et al., 2022). This good consistency demonstrates the reliability of the ALT-TG method in estimating VLM. The ALT-TG method proves to be a robust alternative for estimating coastal VLM, particularly in regions where GNSS data are limited or unavailable.

Table 4 shows that the maximum and average absolute differences between the ALT-TG method, considering optimal noise characteristics, and the GNSS results are 1.79 mm/a and 0.79 mm/a, respectively, with a SD of 0.44 mm/a. This indicates

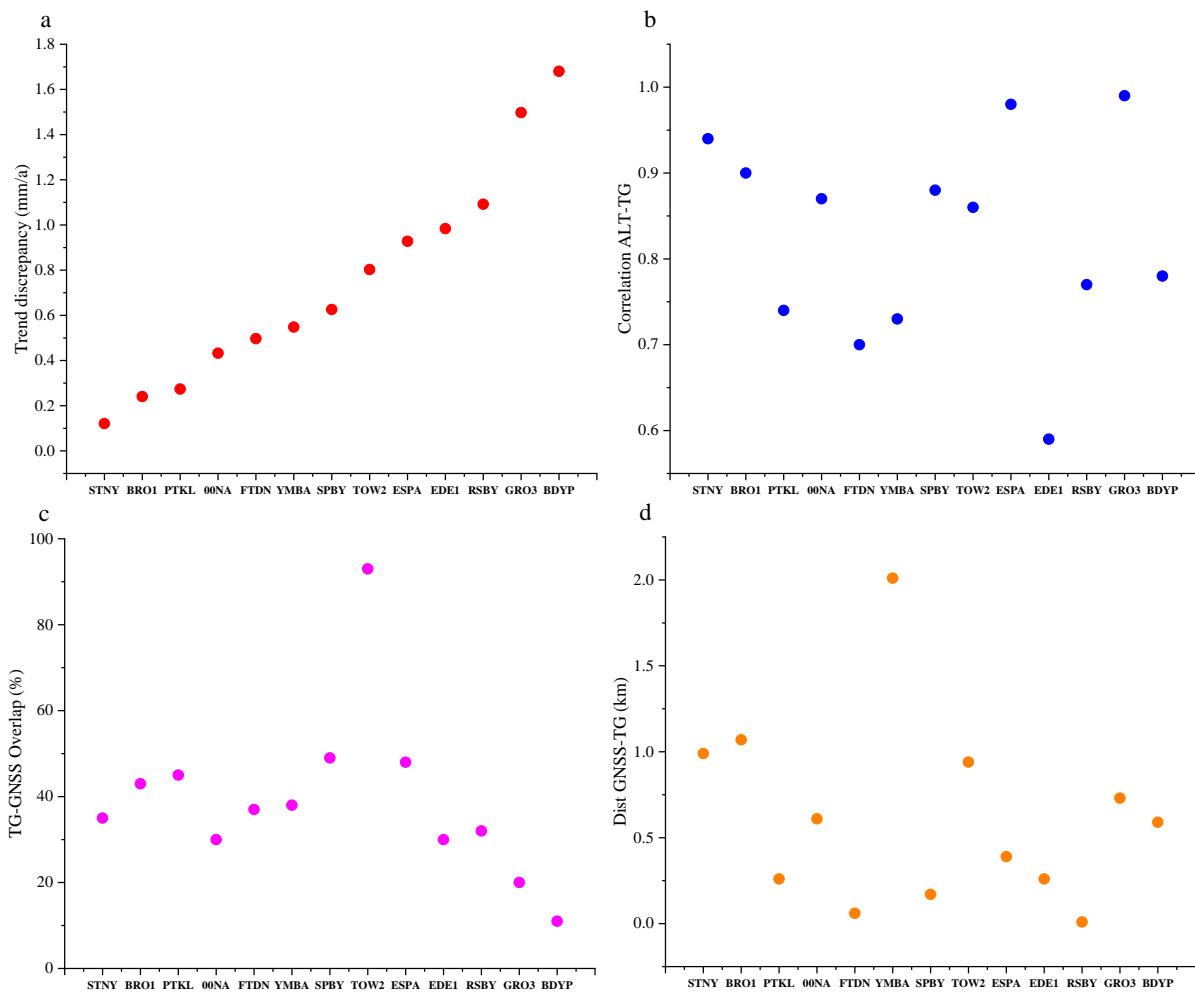


**Fig. 8** Potential Factors Affecting the Comparison of Results Produced by Different Techniques.

smaller differences compared to the results calculated from the two official GNSS data sources. This further emphasizes the necessity of considering noise characteristics in estimating coastal VLM trends, enabling the mitigation of the influence of time series noise and improving the accuracy of VLM trend estimates. Comparison results demonstrate a good consistency between the VLM trends calculated using the ALT-TG method and those using the three GNSS methods, affirming the suitability of ALT-TG for inverting VLM in coastal zones. Furthermore, the root means square error (RMSE) discrepancies between the weighted GNSS data from different institutions and the ALT-TG results are further reduced, indicating that the VLM measurements from weighted GNSS data are more reliable. Based on these findings, we conclude that both methods can effectively estimate coastal VLM. To further explore the factors influencing the differences between ALT-TG and GNSS-calculated VLM, we analyzed the absolute differences between the ALT-TG results and the weighted GNSS results, as shown in Figure 8.

With the dataset, we tried to further test the relation between the discrepancies found in Figure 8a and a number of factors that potentially affect the inter-technique comparison. We considered the correlation between SA and TG time series (Fig. 8b), the length and overlap of the different time series (Fig. 8c), and the distance between measurement points (Fig. 8d), but no clear correlations appeared. When a relevant discrepancy is observed, it is often possible to identify a parameter or a group of parameters that are likely responsible, but each case has to be considered independently on a station-by-station basis. To facilitate the establishment of connections between the data, we normalized the data and conducted correlation analysis with the data in Figure 8a. We found that, in most cases, the only parameter beneficial for comparison is a long overlapping period between the GNSS and the TG time series (the correlation coefficient between Figure 8c and Figure 8a is -0.41). Other influencing factors showed a weaker connection with the differences in VLM estimates calculated by different

techniques. This situation is reasonable. For example, the BDYP and GRO3 sites exhibit significant differences between the VLM trends estimated by the ALT-TG and GNSS methods due to the short GNSS time series at these sites (see Table 1 and Figure 6). This short duration of GNSS observations results in a lower overlap between the two methods, leading to relatively larger differences in the calculated VLM trends. This is in the agreement with findings by Santamaría-Gómez et al. (2017), who identified the limited length of the time series (together with reference frame issues) as a prominent source of uncertainty for the characterization of VLM at TG sites with GNSS observations.

In conclusion, the ALT-TG method can serve as an alternative for monitoring coastal VLM, particularly benefiting areas with shorter GNSS time series or sites located farther from the coastline. However, the use of ALT-TG for VLM calculation is not devoid of errors. For example, oceanic signal contamination of the SA and TG sequences at some sites, as well as differences in instrument calibration between the two datasets, can introduce biases in the results. Therefore, when there is a significant discrepancy between ALT-TG and GNSS results, a more detailed assessment is required to identify the source of this difference and to determine whether the ALT-TG results can be considered reliable.

#### 4. CONCLUSIONS

The main purpose of this study is to estimate the VLM of 13 TG sites along the Australian coast by combining SA and TG. Additionally, these estimates are compared with the vertical velocity calculations from nearby GNSS stations. The following summarizes the main content of the article:

1. Absolute and RSL changes along the Australian coast: Utilizing data recorded by SA and TG from 1993 to 2021, the study estimated sea level trends considering the influence of time-varying noise on rate estimates using three different noise models (ARMA, ARFIMA, GGM). The sea level rate of each site was obtained based on the BIC<sub>tp</sub> criterion with optimal noise model. The results indicate that the ASL change rate at these sites are all smaller than the RSL change rate, with an average ASL change trend of  $3.01 \pm 0.57$  mm/a, significantly different from the average RSL change trend of  $4.61 \pm 2.00$  mm/a, with a difference of 1.60 mm/a, reflecting the significant impact of VLM on Australian coastline.
2. GNSS vertical rate estimation: Considering the GNSS trend estimates under the optimal noise model, the study estimated the VLM velocity based on the time series of GNSS stations adjacent to TG sites and compared them with official data from NGL and SONEL, found a good consistency among the three datasets. From the solutions analyzed as part of this study, the root means square error (RMSE) were determined to

be 0.40, 0.43, and 0.58 mm/a for OUR, SONEL, and NGL, respectively.

3. ALT-TG inversion of VLM: Comparing the VLM values inverted by ALT-TG with the values weighted by the trends estimated from three GNSS sources, The analysis showed that the average absolute difference between the two methods is 0.75 mm/a, with an RMSE of 0.88 mm/a, this is considerably less than previous studies (Ray et al., 2010; Ostanciaux et al., 2012; Pfeffer et al., 2016), likely due to the use of longer data records and more appropriate noise modeling methods. This demonstrates the feasibility of using ASL and TG data to invert the VLM along coastlines. Under conditions of high-quality SA and TG datasets, neglecting instrument errors and ignoring factors such as oceanic signals, the ALT-TG method can serve as an alternative for estimating coastal VLM. This mitigates the disadvantage of inaccurate VLM estimation caused by short GNSS time series or sites far from the coastline, providing an alternative method for monitoring coastal VLM.
4. Sources of VLM estimation differences: Analyzing the source of differences in VLM obtained by ALT-TG and GNSS methods, it was found that the difference between the two techniques is significantly related to the time overlap scale of ALT-TG and GNSS datasets. In regions with high observation quality and reliable data sources (provided that no sudden inter-technique offsets occur), the length of the overlap period between TG and GNSS observations is the most important parameter influencing the consistency of trends between the two techniques.

#### ACKNOWLEDGMENTS

This work was sponsored by National Natural Science Foundation of China (42364002), Major Discipline Academic and Technical Leaders Training Program of Jiangxi Province (20225BCJ23014), The Key Research and Development Program Project of Jiangxi Province (20243BBI91033), Jiangxi Province 2024 Graduate Innovation Special Fund Project (YC2024-5552, YC2024-S553).

#### DECLARATION OF COMPETING INTEREST

The authors declare that they have no known competing financial interests or personal relationships that could have appeared to influence the work reported in this paper.

#### REFERENCES

- Altamimi, Z., Collilieux, X., Legrand, J., Garayt, B. and Boucher, C.: ITRF2005, 2007, A new release of the International Terrestrial Reference Frame based on time series of station positions and Earth Orientation Parameters. *J. Geophys. Res., Solid Earth*, 112, B9. DOI: 10.1029/2007JB004949

- Avsar, N.B., Jin, S., Kutoglu, H. and Gurbuz, G.: 2016, Sea level change along the Black Sea coast from satellite altimetry, tide gauge and GPS observations. *Geod. Geodyn.*, 7, 50–55. DOI: 10.1016/j.geog.2016.03.005
- Adebisi, N., Balogun, A.L., Min, T.H. and Tella, A.: 2021, Advances in estimating Sea Level Rise: A review of tide gauge, satellite altimetry and spatial data science approaches. *Ocean Coast. Manag.*, 208, 105632. DOI: 10.1016/j.ocecoaman.2021.105632
- Avsar, N.B., Jin, S., Kutoglu, S.H. and Gurbuz, G.: 2017, Vertical land motion along the Black Sea coast from satellite altimetry, tide gauges and GPS. *Adv. Space Res.*, 60, 2871–2881. DOI: 10.1016/j.asr.2017.08.012
- Bitharis, S. et al.: 2017, The role of GNSS vertical velocities to correct estimates of sea level rise from tide gauge measurements in Greece. *Mar. Geod.*, 40, 297–314. DOI: 10.1080/01490419.2017.1322646
- Blewitt, G., Hammond, W.C. and Kreemer, C.: 2018, Harnessing the GPS data explosion for interdisciplinary science. *Eos*, 99. DOI: 10.1029/2018EO104623
- Blewitt, G., Kreemer C., Hammond W. and Gazeaux, J.: 2016, MIDAS robust trend estimator for accurate GPS station velocities without step detection. *J. Geophys. Res., Solid Earth*, 121, 3, 2054–2068. DOI: 10.1002/2015JB012552
- Bos, M.S., Fernandes, R.M.S., Williams, S.D.P. and Bastos, L.: 2012, Fast error analysis of continuous GNSS observations with missing data. *J. Geod.*, 87, 351–360. DOI: 10.1007/s00190-012-0605-0
- Bos, M.S., Williams, S.D.P., Araújo, I.B. and Bastos, L.: 2014, The effect of temporal correlated noise on the sea level rate and acceleration uncertainty. *Geophys. J. Int.*, 196, 1423–1430. DOI: 10.1093/gji/ggt481
- Beckley, B.D. et al.: 2010, Assessment of the Jason-2 extension to the TOPEX/Poseidon, Jason-1 sea-surface height time series for global mean sea level monitoring. *Mar. Geod.*, 33, S1, 447–471. DOI: 10.1080/01490419.2010.491029
- Bruni, S., Fenoglio, L., Raicich, F. and Zerbini, S.: 2022, On the consistency of coastal sea-level measurements in the Mediterranean Sea from tide gauges and satellite radar altimetry. *J. Geod.*, 96, 6, 41. DOI: 10.1007/s00190-022-01626-9
- Burgette, R.J. et al.: 2013, Characterizing and minimizing the effects of noise in tide gauge time series: relative and geocentric sea level rise around Australia. *Geophys. J. Int.*, 194, 719–736. DOI: 10.1093/gji/ggt131
- Brown, S., Nicholls, R.J., Woodroffe, C. D., Hanson, S., Hinkel, J., Kebede, A.S., ... Vafeidis, A.T.: 2013, Sea-level rise impacts and responses: a global perspective. In: Finkl, C. (ed.), *Coastal Hazards*, Coastal Research Library, 1000. Springer, Dordrecht, 117–149. DOI: 10.1007/978-94-007-5234-4\_5
- Cazenave, A. et al.: 1999, Sea level changes from Topex-Poseidon altimetry and tide gauges, and vertical crustal motions from DORIS. *Geophys. Res. Lett.*, 26, 2077–2080. DOI: 10.1029/1999GL900472
- Church, J.A. and White, N.J.: 2006, A 20th century acceleration in global sea-level rise. *Geophys. Res. Lett.*, 33, 1. DOI: 10.1029/2005GL024826
- Church, J.A. and White, N.J.: 2011, Sea-level rise from the late 19th to the early 21st century. *Surv. Geophys.*, 32, 585–602. DOI: 10.1007/s10712-011-9119-1
- Church, J.A. et al.: 2013, Sea level change. In: *IPCC Climate Change 2013: The Physical Science Basis*, chap. 13, edited by T. F. Stocker et al., Cambridge Univ. Press, Cambridge, U.K., and New York.
- Collilieux, X. and Wöppelmann, G.: 2011, Global sea-level rise and its relation to the terrestrial reference frame. *J. Geod.*, 85, 9–22. DOI: 10.1007/s00190-010-0412-4
- Denys, P.H., Beavan, R.J., Hannah, J., Pearson, C.F., Palmer, N., Denham, M. and Hreinsdottir, S.: 2020, Sea level rise in New Zealand: The effect of vertical land motion on century-long tide gauge records in a tectonically active region. *J. Geophys. Res., Solid Earth*, 125, 1. DOI: 10.1029/2019JB018055
- Donner, R.V. et al.: 2012, Spatial patterns of linear and nonparametric long-term trends in Baltic sea-level variability. *Nonlinear Process. Geophys.* 19, 1, 95–111. DOI: 10.5194/npg-19-95-2012
- Fu, L.-L. and Cazenave, A. (eds.): 2000, *Satellite altimetry and earth sciences: A handbook of techniques and applications*. Elsevier.
- Grgić, M., Bender, J. and Bašić, T.: 2020, Estimating vertical land motion from remote sensing and in-situ observations in the Dubrovnik area (Croatia): A multi-method case study. *Remote Sens.*, 12, 21, 3543. DOI: 10.3390/rs12213543
- Hamlington, B.D. et al.: 2020, Understanding of contemporary regional sea-level change and the implications for the future. *Rev. Geophys.*, 58, 3, e2019RG000672. DOI: 10.1029/2019RG000672
- Hammond, W.C., Blewitt, G., Kraemer, C. and Nerem, R.S.: 2021, GPS imaging of global vertical land motion for studies of sea level rise. *J. Geophys. Res., Solid Earth.*, 126, 7, e2021JB022355. DOI: 10.1029/2021JB022355
- Harvey, T.C., Hamlington, B.D., Frederikse, T. et al.: 2021, Ocean mass, sterodynamic effects, and vertical land motion largely explain US coast relative sea level rise. *Commun. Earth Environ.*, 2, 1, 233. DOI: 10.1038/s43247-021-00300-w
- Hay, C.C., Morrow, E., Kopp, R.E. and Mitrovica, J.X.: 2015, Probabilistic reanalysis of twentieth-century sea-level rise. *Nature.*, 517, 481–484. DOI: 10.1038/nature14093
- He, X., Montillet, J.P., Fernandes, R., Bos, M., Yu, K., Hua, X. and Jiang, W.: 2017, Review of current GPS methodologies for producing accurate time series and their error sources. *J. Geodyn.*, 106, 12–29. DOI: 10.1016/j.jog.2017.01.004
- He, X., Bos, M.S., Montillet, J.P. and Fernandes, R.M.S.: 2019, Investigation of the noise properties at low frequencies in long GNSS time series. *J. Geod.*, 93, 1271–1282. DOI: 10.1007/s00190-019-01244-y
- He, X. et al.: 2022, Sea level rise estimation on the Pacific coast from southern California to Vancouver Island. *Remote Sens.*, 14, 17, 4339. DOI: 10.3390/rs14174339
- Holgate, S. et al.: 2013, New data systems and products at the permanent service for mean sea level. *J. Coast. Res.*, 29, 493–504. DOI: 10.2307/23486334
- Huang, J. et al.: 2024, Enhancing sea level rise estimation and uncertainty assessment from satellite altimetry through spatiotemporal noise modeling. *Remote Sens.*, 16, 8, 1334. DOI: 10.3390/rs16081334

- Hughes, C.W. and Williams, S.D.P.: 2010, The color of sea level: Importance of spatial variations in spectral shape for assessing the significance of trends. *J. Geophys. Res., Oceans.*, 115, C10. DOI: 10.1029/2010JC006102
- King, M.A. et al.: 2010, Improved constraints on models of glacial isostatic adjustment: A review of the contribution of ground-based geodetic observations. *Surv. Geophys.*, 31, 465–507. DOI: 10.1007/s10712-010-9100-4
- King, M.A., Keshin, M., Whitehouse, P.L., Thomas, I.D., Milne, G. and Riva, R.E.: 2012, Regional biases in absolute sea-level estimates from tide gauge data due to residual unmodeled vertical land movement. *Geophys. Res. Lett.*, 39, 14. DOI: 10.1029/2012GL052348
- Kleinherenbrink, M., Riva, R. and Frederikse, T.: 2018, A comparison of methods to estimate vertical land motion trends from GNSS and altimetry at tide gauge stations. *Ocean Sci.*, 14, 187–204. DOI: 10.5194/os-14-187-2018
- Kowalczyk, K., Pajak, K., Wieczorek, B. and Naumowicz, B.: 2021, An analysis of vertical crustal movements along the European coast from satellite altimetry, tide gauge, GNSS and radar interferometry. *Remote Sens.*, 13, 11, 2173. DOI: 10.3390/rs13112173
- Li, X., Barriot, J.-P., Ducarme, B., Hopuare, M. and Lou, Y.: 2024, Monitoring absolute vertical land motions and absolute sea-level changes from GPS and tide gauges data over French Polynesia. *Geod. Geodyn.*, 15, 13–26. DOI: 10.1016/j.geog.2023.02.007
- Lyon, T.J., Filmer, M.S. and Featherstone, W.E.: 2018, On the use of repeat leveling for the determination of vertical land motion: Artifacts, aliasing, and extrapolation errors. *J. Geophys. Res., Solid Earth.*, 123, 7021–7039. DOI: 10.1029/2018JB015705
- Marcos, M. et al.: 2019, Coastal sea level and related fields from existing observing systems. *Surv. Geophys.*, 40, 1293–1317. DOI: 10.1007/s10712-019-09513-3
- Montillet, J.-P., Melbourne, T.I. and Szeliga, W.M.: 2018, GPS vertical land motion corrections to sea-level rise estimates in the Pacific Northwest. *J. Geophys. Res., Oceans*, 123, 6, 1196–1212. DOI: 10.1002/2017JC013257
- Nerem, R.S. and Mitchum, G.T.: 2002, Estimates of vertical crustal motion derived from differences of TOPEX/POSEIDON and tide gauge sea level measurements. *Geophys. Res. Lett.*, 29, 19, 40-1–40-4. DOI: 10.1029/2002GL015037
- Oelmann, J., Marcos, M., Passaro, M., Sanchez, L., Dettmering, D., Dangendorf, S. and Seitz, F.: 2024, Regional variations in relative sea-level changes influenced by nonlinear vertical land motion. *Nat. Geosci.*, 17, 2, 137–144. DOI: 10.1038/s41561-023-01357-2
- Oelmann, J., Passaro, M., Sánchez, L., Dettmering, D., Schwatke, C. and Seitz, F.: 2022, Bayesian modelling of piecewise trends and discontinuities to improve the estimation of coastal vertical land motion. *J. Geod.*, 96, 9. DOI: 10.31223/X5GP92
- Ostanciaux, É., Husson, L., Choblet, G., Robin, C. and Pedoja, K.: 2012, Present-day trends of vertical ground motion along the coast lines. *Earth-Sci. Rev.*, 110, 1, 74–92. DOI: 10.1016/j.earscirev.2011.10.004
- Passaro, M., Müller, F.L., Oelmann, J., Rautiainen, L., Dettmering, D., Hart-Davis, M.G., Abulaitijiang, A., Andersen, O.B., Hoyer, J.L., Madsen, K.S. and Ringgaard, I.M.: 2021, Absolute Baltic sea level trends in the satellite altimetry era: A revisit. *Front. Mar. Sci.*, 8, 647607. DOI: 10.3389/fmars.2021.647607
- Peltier, W.R., Argus, D.F. and Drummond, R.: 2015, Space geodesy constrains ice age terminal deglaciation: The global ICE-6G\_C (VM5a) model. *J. Geophys. Res., Solid Earth.*, 120, 450–487. DOI: 10.1002/2014JB011176
- Peng, F., Deng, X. and Cheng X.: 2022, Australian coastal sea level trends over 16 yr of reprocessed Jason Altimeter 20-Hz Data Sets. *J. Geophys. Res., Oceans*, 127, 3, e2021JC018145. DOI: 10.1029/2021JC018145
- Pfeffer, J. and Allemand, P.: 2016, The key role of vertical land motions in coastal sea level variations: A global synthesis of multisatellite altimetry, tide gauge data and GPS measurements. *Earth Planet. Sci. Lett.*, 439, 39–47. DOI: 10.1016/j.epsl.2016.01.027
- PSMSL Permanent Service for Mean Sea Level: 2023 Data. <https://www.psmsl.org/data/>. Accessed June 2023.
- Qiao, X., Chu, T., Tissot, P., Ali, I. and Ahmed, M.: 2023, Vertical land motion monitored with satellite radar altimetry and tide gauge along the Texas coastline, USA, between 1993 and 2020. *Int. J. Appl. Earth Obs. Geoinf.*, 117, 103222. DOI: 10.1016/j.jag.2023.103222
- Ray, R.D., Beckley, B.D. and Lemoine, F.G.: 2010, Vertical crustal motion derived from satellite altimetry and tide gauges, and comparisons with DORIS measurements. *Adv. Space Res.*, 45, 12, 1510–1522. DOI: 10.1016/j.asr.2010.02.020
- Ribal, A. and Young, I.R.: 2019, 33 years of globally calibrated wave height and wind speed data based on altimeter observations. *Sci. Data*, 6, 1, 77. DOI: 10.1038/s41597-019-0083-9
- Rovere, A., Stocchi, P. and Vacchi, M.: 2016, Eustatic and relative sea level changes. *Curr. Clim. Change Rep.*, 2, 221–231. DOI: 10.1007/s40641-016-0045-7
- Royston, S. et al.: 2018, Sea-level trend uncertainty with Pacific climatic variability and temporally-correlated noise. *J. Geophys. Res., Oceans*, 123, 3, 1978–1993. DOI: 10.1002/2017JC013655
- Santamaría-Gómez, A. et al.: 2012, Mitigating the effects of vertical land motion in tide gauge records using a state-of-the-art GPS velocity field. *Glob. Planet. Change.*, 98-99, 8, 6–17. DOI: 10.1016/j.gloplacha.2012.07.007
- Santamaría-Gómez, A. et al.: 2017, Uncertainty of the 20th century sea-level rise due to vertical land motion errors. *Earth Planet. Sci. Lett.*, 473, 24–32. DOI: 10.1016/j.epsl.2017.05.038
- Santamaría-Gómez, A., Gravelle, M. and Wöppelmann, G.: 2014, Long-term vertical land motion from double-differenced tide gauge and satellite altimetry data. *J. Geod.*, 88, 207–222. DOI: 10.1007/s00190-013-0677-5
- Taburet, G. et al.: 2019, DUACS DT2018: 25 years of reprocessed sea level altimetry products. *Ocean Sci.*, 15, 5, 1207–1224. DOI: 10.5194/os-15-1207-2019

- Takagi, H., Thao, N.D. and Anh, L.T.: 2016, Sea-level rise and land subsidence: impacts on flood projections for the Mekong Delta's largest city. *Sustainability*, 8, 9, 959. DOI: 10.3390/su8090959
- Tay, C., Lindsey, E.O., Chin, S.T., McCaughey, J.W., Bekaert, D., Nguyen, M., Hua, H., Manipon, G., Karim, M., Horton, B.P. and Li, T.: 2022, Sea-level rise from land subsidence in major coastal cities. *Nat. Sustain.*, 5, 12, 1049–1057. DOI: 10.1038/s41893-022-00947-z
- Thompson, P.R., Hamlington, B.D., Landerer, F.W. and Adhikari, S.: 2016, Are long tide gauge records in the wrong place to measure global mean sea level rise? *Geophys. Res. Lett.*, 43, 19. DOI: 10.1002/2016GL070552
- Tiampo, K.F., Mazzotti, S. and James, T.S.: 2012, Analysis of GPS measurements in Eastern Canada using principal component analysis. *Pure Appl. Geophys.*, 169, 1483–1506. DOI: 10.1007/s00024-011-0420-1
- Wang, J., Church, J. A., Zhang, X. and Chen, X.: 2021 reconciling global mean and regional sea level change in projections and observations. *Nat. Commun.*, 12, 990. DOI: 10.1038/s41467-021-21265-6
- Wang, J., Yi, S., Li, M., Wang, L. et al.: 2018, Effects of sea level rise, land subsidence, bathymetric change and typhoon tracks on storm flooding in the coastal areas of Shanghai. *Sci. Total Environ.*, 621, 6183, 228–234. DOI: 10.1016/j.scitotenv.2017.11.224
- Watson, P.J.: 2019, An assessment of the utility of satellite altimetry and tide gauge data (ALT-TG) as a proxy for estimating vertical land motion. *J. Coas. Res.*, 35, 6, 1131–1144. DOI: 10.2112/JCOASTRES-D-19-00031.1
- Watson, C.S. et al.: 2015, Unabated global mean sea-level rise over the satellite altimeter era. *Nat. Clim. Change.*, 5, 6, 565–568. DOI: 10.1038/nclimate2635
- White, N.J. et al.: 2014, Australian sea levels - Trends, regional variability and influencing factors. *Earth-Sci. Rev.*, 136, 155–174. DOI: 10.1016/j.earscirev.2014.05.011
- Williams, S.D.P.: 2003, The effect of coloured noise on the uncertainties of rates estimated from geodetic time series. *J. Geod.*, 76, 483–494. DOI: 10.1007/s00190-002-0283-4
- Wöppelmann, G. and Marcos, M.: 2016, Vertical land motion as a key to understanding sea level change and variability. *Rev. Geophys.*, 54, 1, 64–92. DOI: 10.1002/2015RG000502
- Wöppelmann, G. and Marcos, M.: 2012, Coastal sea level rise in southern Europe and the nonclimate contribution of vertical land motion. *J. Geophys. Res., Oceans*, 117, C1. DOI: 10.1029/2011JC007469